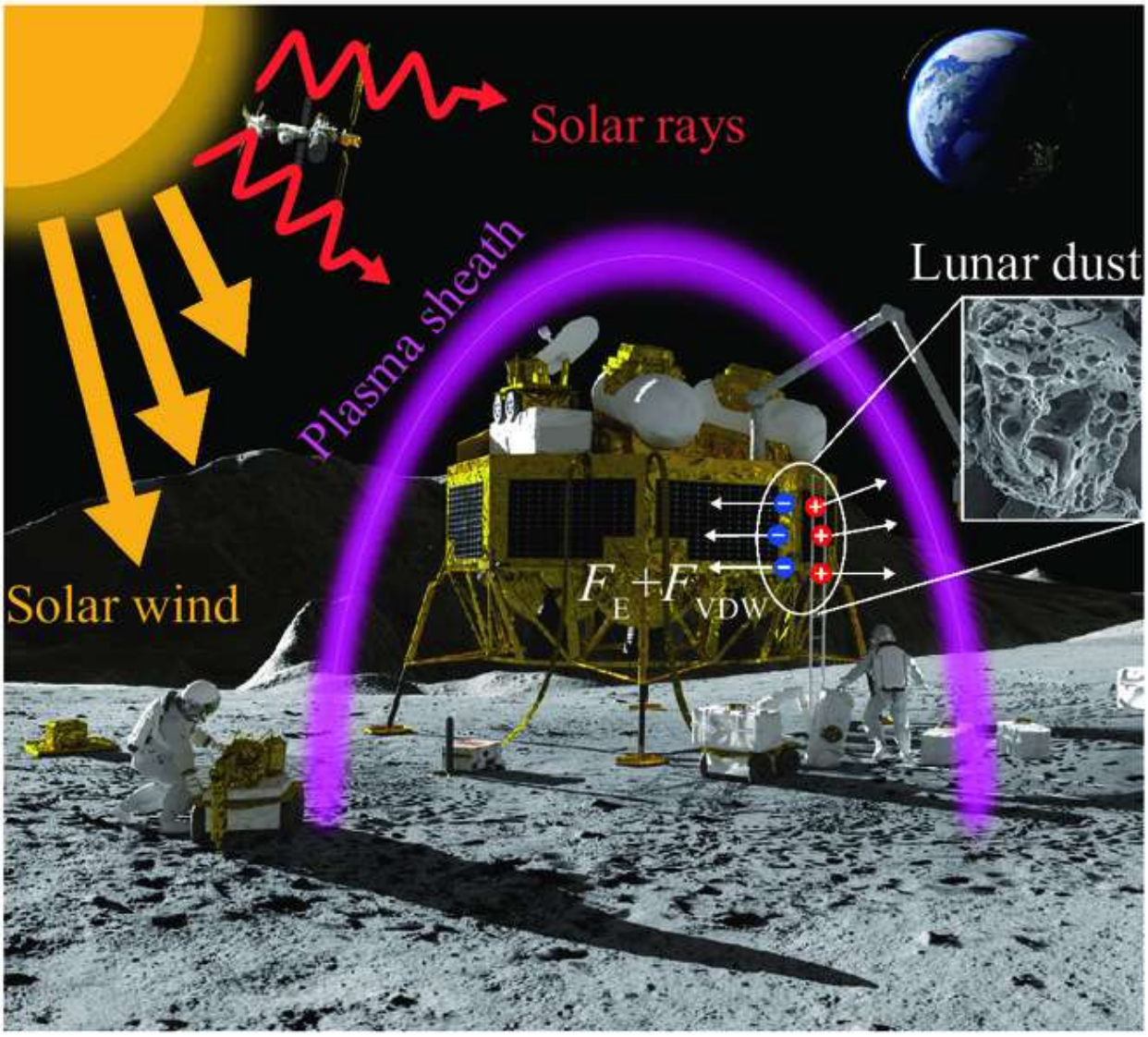

A diagram illustrating the phenomenon of charged dust particles being attracted or repulsed to the charged spacecraft on the lunar surface. Background image republished from ESA-ATG [ESA-ATG. Artist's impression of a Moon exploration scenario.

Understanding The Plasma Sheath with a Review of Chandrayaan-3 Lander/Rover Mission

Ronald H. Freeman, PhD
Space Operations & Support Technical Committee, AIAA

Abstract
Lunar dust mitigation (DM) proposals prominently address issues of wheel-regolith turbocharging and dust levitation from surface regolith that risk-manage safety hazards. However, DM proposals have been less specialized regarding non-regolith exosphere of a "dusty plasma" environment. This paper aims to investigate the dusty plasma exosphere and the photoelectric plasma structures formed therein as they interact with spacecraft and affect

performance of lunar operations. The paper additionally reviews simulation findings of India's successful lander-rover mission (August, 2023), Chandrayaan-3.

Keywords. Dusty plasma, plasma sheath

Introduction

A plasma sheath forms on the night side of the Moon when exposed to highly energetic ambient plasma. Calculations indicate that secondary electron emission (SEE) due to highly energetic plasma electrons leads to the formation of the inverse sheath around the positively charged lunar surface on the night side, where a traditional Debye sheath with a high negative surface potential is anticipated [1].To provide a comprehensive description of the adhesion or escape behavior of dust particles from the sheath, a dynamic model explains the low-velocity collision between charged dust particles and spacecraft enveloped by the plasma sheath. The model further indicates the electrostatic force of a polarized dust particle (based on the image multipole method), and the contact force (calculated using Thornton's adhesive–elastic–plastic collision model). The impact of crucial characteristics of spacecraft and particles, including initial velocity, interface energy, and spacecraft potential, on the dynamic process has been investigated. Due the same charging environment inside the plasma sheath, the vehicle is assumed to be equipotential with the lunar surface.

	Solar illumination (SZA: 180° to 0°) [48]	Lunar plasma wake	Magnetotail lobe	Plasma sheet
Lunar surface potential	−100 to 20 V	−200 to 0 V	−150 to 0 V	−1,000 to 0 V

Table 1. Typical lunar surface potentials **[2].** SZA, solar zenith angle

In this case, the dust particles, oppositely charged with respect to the charged spacecraft, undergo the attractive forces of long-range electrostatic force (F_E) and short-range van der Waals force (F_{VDW}), which cause them to migrate toward the spacecraft surface and ultimately adhere. On the other hand, if the dust particles were to carry the same polarity of charge as the charged spacecraft, they would be acted upon by the repulsive electrostatic forces. Due to the screen effect of the plasma, charged dust particles located outside the edge of sheath do not participate in the electrostatic interaction with the spacecraft. When lunar dust does enter inside the plasma sheath, Das *et al.* (2016) [3] explained the ion drag force and neutral drag force caused by the plasma are negligibly smaller than the electrostatic force. Therefore, charged particles interact with the spacecraft within the confines of the plasma sheath, while the interaction between dust with plasma, neglected.

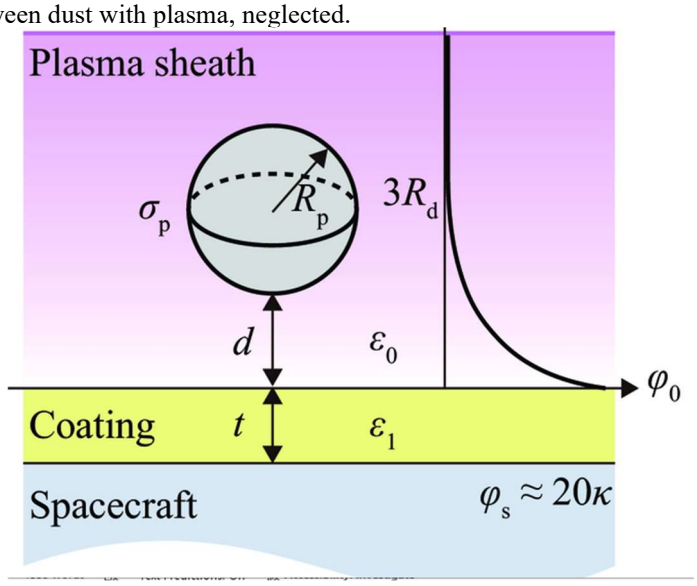

Fig. 2. Geometric representation of a charged dust particle positioned above

a spacecraft surface with a coating layer.

Considering the significant difference in size between the vehicle and the dust particle, the vehicle represents an infinite conducting plane coated with a dielectric layer A and the dust particle (characterized by its radius R_p, uniform surface charge density σ_p, and permittivity ε_p) is positioned at a distance d above the surface. The isolated conductor coating has an insulating dielectric material of thickness t and permittivity ε_1. The boundary of the sheath is simplistically represented as an equipotential conducting shell. The distance between the surface of the coating and the shell is triple the Debye length (R_d) of plasma sheath. The potential of the shell, also known as the plasma spatial potential, is denoted by κ and is usually defined as the reference potential. The floating potential of spacecraft is represented as φ_s. Notably, the decay of potential in the sheath follows an exponential pattern. Owing to the charged spacecraft, an electric field is produced between the surface of the spacecraft and the plasma. This electric field exerts a force on the charged dust particle that is present within the plasma sheath. Figure 3 offers an insight into the effect of spacecraft potential on electrostatic force applied on the particle positioned above the surface of a spacecraft. When a particle carries a positive charge, it is drawn toward the negatively charged spacecraft across the entire range of plasma sheath [4], as illustrated in Fig. 3A.

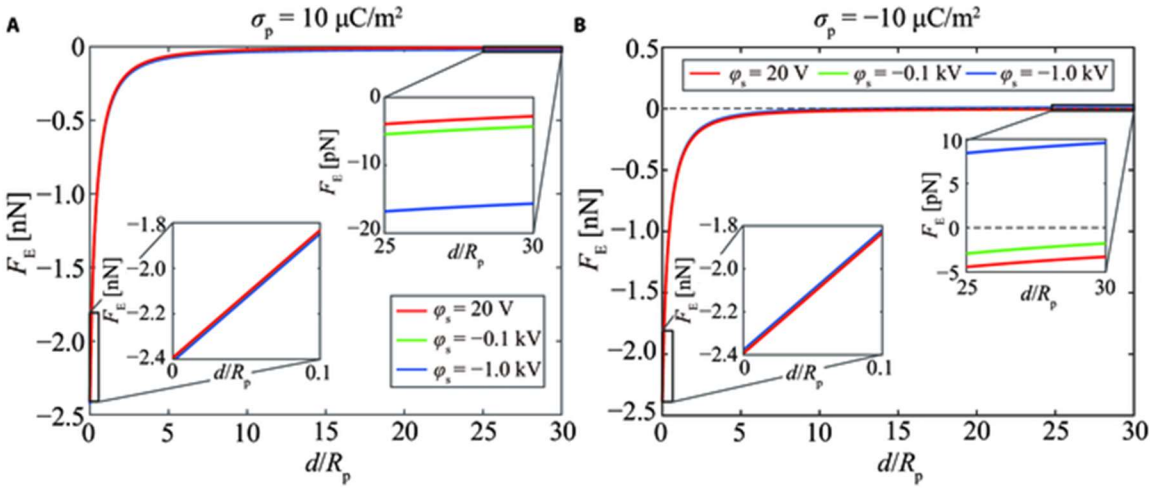

Fig. 3. Electrostatic force F_E versus the dimensionless distance d/R_p for different spacecraft potentials, assuming $\varepsilon_p = 3\varepsilon_0$, $R_p = 10$ μm, $\varepsilon_1 = 3.5\varepsilon_0$, and $t = 125$ μm. The particle carries (A) positive charges and (B) negative charges.

It is important to acknowledge that the final adhesion of particles to the spacecraft is not solely determined by the initial collision. Figure 4 illustrates the trajectory diagrams of particles with positive and negative charge with different initial velocity v_0. These particles originate from the edge of the plasma sheath. The edge of the plasma sheath is defined as the initial position of particles to present the issue of particle adhesion and escape. In this study, it is assumed that the charged dust particle does not exhibit any interaction with the surrounding plasma sheath. For a positively charged particle, it experiences electrostatic attraction within the sheath [5]. When the particle exhibits a low initial velocity, it will promptly adhere to the surface, following trajectory ①. However, in the event that the residual kinetic energy after the initial impact does not surpass the work performed by the electrostatic force, the particle remains incapable of overcoming the electrostatic pull of the spacecraft, resulting in its adherence to the surface after a finite number of collisions (trajectory ②. Only when the initial velocity v_0 increases to the critical escape velocity can the particle successfully overcome the attraction of the spacecraft and break free from the sheath (trajectory ③.

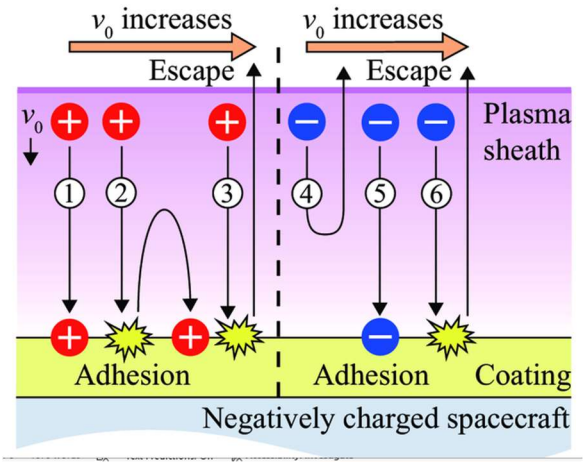

Fig. 4. Diagram illustrating that the adhesion and escape trajectories of positively and negatively charged particles interacted with negative spacecraft potential.

If the initial kinetic energy is insufficient to exceed the work done by the repulsive force, the particle will not come into contact with the spacecraft trajectory ④. With a progressively higher initial velocity, once the velocity v_0 reaches the critical adhesion velocity, the particle has the capability to adhere to the surface of the spacecraft after the collision (trajectory ⑤). However, if the initial velocity v_0 surpasses the critical escape velocity, the remaining kinetic energy will exceed the work performed by the attractive force. As a result, the particle will successfully escape, following trajectory ⑥. Adhesion to the surface occurs only when the initial velocity of a negatively charged particle is within the range of the critical adhesion and escape velocities [6].

Reducing the interface energy of the coating decreases adhesive energy loss, thereby increasing the rebound velocity. However, it is observed that the application of a low-interface-energy coating does not lead to a significant reduction in the critical adhesion velocity. In the absence of external force from active dust removal methods, lowering the interface energy of the dielectric coating does not alleviate the accumulation of dust, which suggests reducing the spacecraft potential as an option [7]. Although the influence of the charged spacecraft's long-range electric field force on the collision process is minimal, it exerts a dominant effect on the trajectory of dust particles within the plasma sheath. The final adhesion or escape state of low velocity charged dust is mainly determined by the electrostatic interaction rather than contact interaction.

Case Study. Charged dust particles and spacecraft surrounded by a plasma sheath.

The Chandrayaan-3 spacecraft landed on the lunar surface on August 23, 2023, marking the first mission to explore near the lunar south pole, a region expected having water ice deposits suitable for harvesting and rocket fuel conversion. The first observations from the ChaSTE payload onboard the lander included

- ChaSTE (Chandra's Surface Thermophysical Experiment) that measured the temperature profile of the lunar topsoil around the pole.

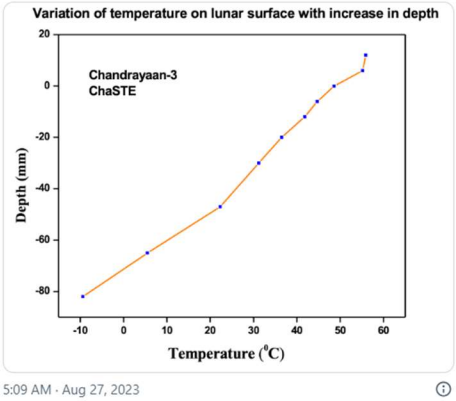

- One experiment measured the temperature of the moon's topsoil at various depths, and ISRO scientist BHM Darukesha told a local news outlet, PTI, that the surface was hotter than expected. "We all believed that the temperature could be somewhere around 20 degrees centigrade to 30 degrees centigrade (68 to 86 degrees Fahrenheit) on the surface, but it is 70 degrees centigrade (158 degrees Fahrenheit). This is surprisingly higher than what we had expected," he said.
- The rover also detected some seismic activity using an instrument designed to measure rumbles and quakes beneath the lunar surface, and the rover used a spectroscope to confirm the presence of sulfur near the moon's south pole.

However long before launched date, Sana & Mishra (2023 simulated a realistic scenario of India's lander-rover mission Chandrayaan-3 and investigated the electric potential development over the Chandrayaan-3 (CH3) landing site under the influence of observed solar ultraviolet/extreme-ultraviolet radiation and real plasma parameters measured by THEMIS as a case study. The electric potential structures coupled with latitude-dependent fermionic photoelectrons, non-Maxwellian plasma electrons, and cold ions. A dynamic variation of the potential structure around the sunlit landing was observed through the analysis. The study predicted a photoelectron density range from 10 to 40 cm^{-3} and mean energy range from 2.6 to 3 eV near the surface of the Chandrayaan-3 landing site, which may be tested by the in-situ measurement [8].

Being an airless body, the Moon is exposed to harsh space plasma conditions, which generates a complex plasma/ electrical environment in the vicinity of the lunar surface. Locally, depending on plasma conditions and solar activities, this electrical environment could be intense and deleterious to the onboard instrument operation and electronics [9]. During the expedition, Ch3 was supposed to reside within this complex plasma environment on the lunar surface. The atmosphere-less lunar surface is directly exposed to energetic UV radiation and solar wind/ambient plasma and undergoes electrostatic charging [10]. And, due to the dominant UV-induced photoemission, the lunar surface generally acquires a positive potential, and a photoelectron sheath forms near the sunlit moon [11].The photoelectron sheath can stretch up to 10–100 m from equator to terminator [12]. Any object residing within this nonneutral space region interacts with the local plasma environment and charged particles within the sheath, which eventually results in a charge development on the object [13]. Moreover, the objects roaming on the charged dusty lunar surface (regolith–wheel interaction) might acquire a huge charge due to frictional (triboelectric) charging and the lack of a significant dissipation mechanism; particularly around the terminator, where photoemission is marginal/absent. Saana and Misha (2023) first discussed and derived the solar zenith angle (sza) at the Ch3 landing site (LS) using the lunar orbital parameters. Other crucial parameters in determining the photoemission current from the lunar surface include incoming solar radiation, work function, photoelectric efficiency χ, and temperature T0 of the lunar surface. To simulate the realistic scenario, data from the ARTEMIS P2 spacecraft (former THEMIS-C probe) were used as an input plasma parameter [14]. The researchers (Saana and Mishra) chose a long time pass between 2013 January 17 and 2013 January 31, covering the typical plasma parameters near the Ch3 LS. The data was later resampled to 1 hr equidistant intervals with a reference time Tf = 2013 January 27 04:30 UTC (date and time of full Moon). Figures 7 and 8 illustrate a typical plasma density and temperature variation near the illuminated Ch3 LS.

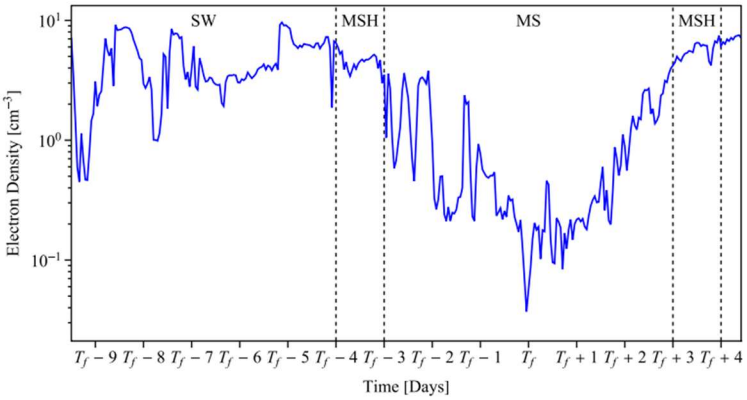

Figure . Sample electron density around the Ch3 LS during the passage measured by the THEMIS-C probe [15]. Here Tf is the time of the full Moon. The vertical lines separate different regions: SW, solar wind; MSH, magnetosheath; MS: inner magnetosphere.

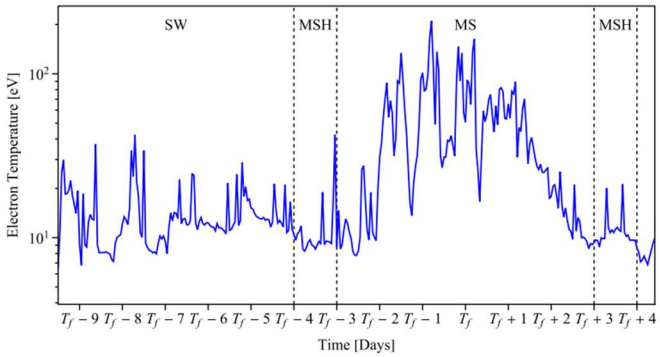

Figure . Sample electron temperature around the Ch3 LS during the passage measured by the THEMIS-C probe [16]. Here Tf refers to the time of the full Moon. The vertical lines separate different regions: SW, solar wind; MSH, magnetosheath; MS: inner magnetosphere.

The sunlit lunar surface undergoes electrostatic charging due to the dynamic interaction between energetic solar radiation and solar wind/ambient plasma collection. The UV-induced photoelectron emission and solar wind/ambient plasma ion collection yield a surface that is positively charged, while the electron collection from the solar wind/ambient plasma makes the surface negatively charged. At any point in time, a finite amount of electric potential is connected with the surface. This surface potential is screened by the emitted photoelectron and ambient plasma constituent forming a photoelectron sheath in the vicinity of the lunar surface [17]. The degree of surface charging varies across different locations on the Moon, leading to the formation of different potential/field structures within the sheath. Nitter (1998) [18]. suggested the possibility of three kinds of potential structures within the sheath; a schematic is illustrated in Figure 4. At the locations with negligible photoemission, the surface has a negative surface potential due to dominant plasma electron collection that altitudinally increases to zero, forming a type C sheath. This is a normal Debye-type potential structure. For significant photoemission, the potential is positive and monotonically decreases to zero to form a type B sheath. The boundary conditions lead to another sheath solution, where the surface potential will decrease to a negative minimum and then increase to zero, giving rise to a nonmonotonic potential structure (type A sheath). These potential structures predicted from solutions to Poisson's equation establish the relationship between the electric potential and the charge population within the photoelectron sheath.

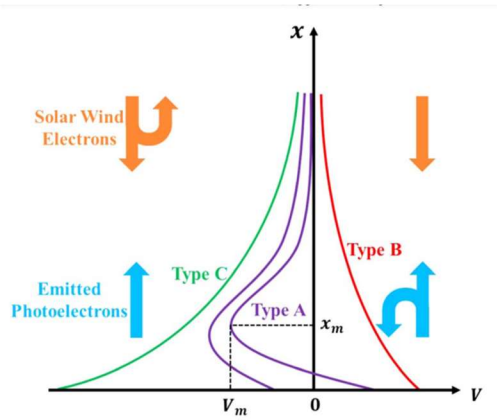

Figure . Different types of sheaths on the lunar surface. Here x refers the altitude, and V is the electric potential. Adapted from Sana & Mishra (2023).

Depending on the type of plasma sheath (as shown in above Figure), there can be up to four different populations of electrons within the sheath. The first two populations are the plasma electrons that interact with the lunar surface and the photoelectrons that escape to infinity. These are referred to as "free plasma electrons" (nsef) and "free photoelectrons" (npef), respectively. The other two populations are the plasma electrons and photoelectrons, which are reflected by a potential barrier within the sheath. These are known as "captured plasma electrons" (nsec) and "captured photoelectrons" (npec), respectively. Other than electrons, positively charged plasma ions (nsi) also

contribute to the photoelectron sheath. Here e is the electronic charge, and ε0 is the permittivity in free space. The surface and dip potential (potential minima) are used as boundary conditions to solve Poisson's equation. Note that the surface and dip potentials depend on the charging currents connected with the lunar surface, which varies temporally with the orbital motion of the Moon.

Conclusion

A plasma sheath forms on the night side of the Moon when exposed to highly energetic ambient plasma. Due to the same charging environment inside the plasma sheath, spacecraft within, is assumed to be equipotential with the lunar surface. Owing to the charged spacecraft, an electric field is produced between the surface of the spacecraft and the plasma. Reducing the interface energy of the spacecraft coating, thereby increases the rebound velocity of dust particles. In the absence of external force from active dust removal methods, lowering the interface energy of the dielectric coating does not alleviate the accumulation of dust, which suggests reducing the spacecraft potential as an option In other words, the final adhesion or escape state of low velocity charged dust is mainly determined by the electrostatic interaction rather than contact interaction.

However long before CH3 launch date, Sana & Mishra (2023) simulated a realistic scenario of India's lander-rover mission and investigated the electric potential development over CH3 landing as a case study. The electric potential structures coupled with latitude-dependent fermionic photoelectrons, non-Maxwellian plasma electrons, and cold ions. A dynamic variation of the potential structure around the sunlit landing was observed through the analysis. The study predicted a photoelectron density range from 10 to 40 cm^{-3} and mean energy range from 2.6 to 3 eV near CH3 surface. Any object residing within this nonneutral space region interacts with the local plasma environment and charged particles within the sheath. Moreover, the objects roaming on the charged dusty lunar surface (regolith–wheel interaction) might acquire a huge charge due to frictional (triboelectric) charging and the lack of a significant dissipation mechanism. Future in-situ measurements are needed for verification.

References

[1] Sana, T. & Mishra, S. (2024). Possibility of inverse sheath in the lunar nightside due to secondary electron emission, *Fundamental Plasma Physics*, *10*.

[2] Halekas, J.,, Delory, G., Lin, R., Stubbs, T., & Farrell, W. (2008). Lunar Prospector observations of the electrostatic potential of the lunar surface and its response to incident currents. *J Geophys Res Space Physics*.,113(A9), A0910**.**

[3] Das G., Deka, R., & Bora M. (2016). Revisiting the plasma sheath–dust in plasma sheath. *Phys Plasmas*., 23, Article 042308.

[4] Feng, Y., Zhou, Z., Wang, R., Han, Y., Tang, X., & Zhao, W. (2024). Modeling of Electrostatic and Contact Interaction between Low-Velocity Lunar Dust and Spacecraft. *Space: Science & Technology*, *4*, 0187.

[5] Feng, Y., Zhou, Z., Wang, R., Han, Y., Tang, X., & Zhao, W. (2024). Modeling of Electrostatic and Contact Interaction between Low-Velocity Lunar Dust and Spacecraft. *Space: Science & Technology*, *4*, 0187.

[6] Feng, Y., Zhou, Z., Wang, R., Han, Y., Tang, X., & Zhao, W. (2024). Modeling of Electrostatic and Contact Interaction between Low-Velocity Lunar Dust and Spacecraft. *Space: Science & Technology*, *4*, 0187.

[7] Zanon, P, Dunn, M, & Brooks G. (2023). Current Lunar dust mitigation techniques and future directions. *Acta Astronaut*., 213, 627–644.

[8] Sana, T. & Mishra, S. (2023). Plasma Sheath around Chandrayaan-3 Landing Site: A Case Study. *The Planetary Science Journal*, *4*(9), 158.

[9] Zakharov, A. V., Zelenyi, L., & Popel', S. (2020). Lunar dust: Properties and potential hazards. *Solar System Research*, *54*, 455-476.

[10] Whipple, F. (1981). *Orbiting the Sun: Planets and Satellites of the Solar System*. Harvard University Press].

[11] Mishra, S. & Bhardwaj, A. (2019). Photoelectron sheath on lunar sunlit regolith and dust levitation. *The Astrophysical Journal*, *884*(1),5.

[12] Sana, T. & Mishra, S. (2023). Plasma Sheath around Chandrayaan-3 Landing Site: A Case Study. *The Planetary Science Journal*, *4*(9), 158.

[13] Farrell, W., Stubbs, T., Halekas, J., Delory, G., Collier, M., Vondrak, R., & Lin, R. (2008). Loss of solar wind plasma neutrality and effect on surface potentials near the lunar terminator and shadowed polar regions. *Geophysical Research Letters*, *35*(5).

[14] Korotova, G., Sibeck, D., Weatherwax, A., Angelopoulos, V., & Styazhkin, V. (2011). THEMIS observations of a transient event at the magnetopause. *Journal of Geophysical Research: Space Physics*, *116*(A7).

[15] Korotova, G., Sibeck, D., Weatherwax, A., Angelopoulos, V., & Styazhkin, V. (2011). THEMIS observations of a transient event at the magnetopause. *Journal of Geophysical Research: Space Physics*, *116*(A7).

[16] Korotova, G., Sibeck, D., Weatherwax, A., Angelopoulos, V., & Styazhkin, V. (2011). THEMIS observations of a transient event at the magnetopause. *Journal of Geophysical Research: Space Physics*, *116*(A7).

[17] Mishra, S. & Bhardwaj, A. (2019). Photoelectron sheath on lunar sunlit regolith and dust levitation. *The Astrophysical Journal*, *884*(1),5.

[18] Nitter, T., Havnes, O., & Melandsø, F. (1998). Levitation and dynamics of charged dust in the photoelectron sheath above surfaces in space. *Journal of Geophysical Research: Space Physics*, *103*(A4), 6605-6620.